International Journal of Concrete Structures and Materials
DOI 10.1186/s40069-018-0253-8
ISSN 1976-0485 / eISSN 2234-1315

Experimental Investigation on Flexural Crack Control for High-Strength Reinforced-Concrete Beam Members

Chien-Kuo Chiu*, Kai-Ning Chi, and Bo-Ting Ho

(Received May 10, 2017, Accepted January 30, 2018)

Abstract: The purpose of this study is to investigate the flexural crack development of high-strength reinforced concrete (HSRC) beams and suggest the design equations of the flexural crack control for HSRC beams. This study conducts two full-size simply-supported beam specimens and seven full-size cantilever beam specimens, and collects the experimental data of twenty full-size simply-supported beams from the past researches. In addition to high-strength reinforced steel bars of specified yielding stresses of 685 and 785 MPa, these specimens are all designed with the high-strength concrete of a specified compressive stress of 70 or 100 MPa. The experimental data is used to verify the application of the flexural crack control equations recommended in ACI 318-14, as reported by AIJ 2010, as reported by JSCE 2007 and as reported by CEB-fib Model Code 2010 on HSRC beam members; then, this study concludes the design equations for the flexural crack control based on ACI 318-14. Additionally, according to the experimental data, to ensure the reparability of an HSRC beam member in a medium-magnitude earthquake, the allowable tensile stress of the main bars can be set at the specified yielding stress of 685 MPa.

Keywords: high-strength reinforced concrete, beam members, flexural crack, serviceability, reparability.

1. Introduction

Over the last six decades, the use of high-strength concrete (HSC) has been gradually transformed with its scope of application as mentioned by the American Concrete Institute (ACI 2010). HSC has a continuously expanding range of applications, owing to its highly favorable characteristics, including the high early age strength, low deformation under the loading owing to its high modulus of elasticity, and high load resistance per unit weight (including shear and moment). HSC is thus very useful for constructing skyscrapers and span suspension bridges. HSC commonly refers to concrete whose compressive strength is at least 60 MPa and less than 130 MPa (FIP/CEB 1990). High-strength reinforcement is increasingly common in the construction industry. In Taiwan, high-strength reinforced concrete (HSRC) includes HRC with a specified compressive strength of at least 70 MPa and high-strength reinforcement with a specified yield strength of at least 685 MPa. As the most commonly applied specification for concrete engineering design in Taiwan, ACI 318-14 (ACI 2014) sets an upper bound of 420 MPa on the yield strength of reinforcing steel bars. Owing to the high strength of concrete and reinforcing steel, the mechanical behavior of HSRC structural members differs from that of normal-strength RC members. Furthermore, few full-scale experimental studies have addressed the mechanical behaviors of HSRC beam and column members. Therefore, mechanical models of HSRC members that accurately capture the lateral force–deformation relationship must be developed since the conventional model of normal-strength RC members may be unfeasible for evaluating the performance of HSRC members or structures.

The Architectural Institute of Japan (AIJ 2010) has stated that building performance is a function of serviceability, safety and reparability. Accordingly, as well as serviceability and safety, the performance-based design of buildings should consider reparability. As a major determinant of the cost of a building over its life cycle, reparability can also be regarded as a basic economic performance metric of a building; its importance has become evident in several seismic disaster events, including the Northridge Earthquake (USA, 1994), the Kobe Earthquake (Japan, 1995), and the Chi–Chi Earthquake (Taiwan, 1999). Obviously, reparability can reduce reconstruction costs after a seismic disaster. Generally, a crack-based damage assessment has a major role in estimating the cost of repairing a building. However, despite various assessments of crack-based damage to RC members or structures, related investigations (Silva et al. 2008; Shimazaki 2009) have focused mainly on normal-

Department of Civil and Construction Engineering, National Taiwan University of Science and Technology, No.43, Keelung Rd., Sec.4, Da'an Dist., Taipei City 10607, Taiwan, ROC.
*Corresponding Author;
E-mail: ckchiu@mail.ntust.edu.tw

Published online: 29 May 2018

strength RC while paying little attention to HSRC structural members. A crack-based damage assessment can also be performed to estimate post-earthquake residual seismic capacity or facilitate performance-based design for a building structure (Soltani et al. 2013; Chiu et al. 2015).

Chiu et al. (2014) and (2016) proposed formulas for determining the allowable stresses of stirrup that ensure the serviceability and reparability of HSRC beam members. However, with respect to controlling flexural cracks of HSRC beam specimens, the development of such cracks must be investigated by performing full-scale experiments. Therefore, in this work, two four-point loading simply-supported beam tests and seven cantilever beam tests are performed, and 20 four-point loading simply-supported beam tests that were performed previously are considered. All specimens herein include a high-strength main reinforcement (with a specified yielding strength of 685 MPa) with high-strength stirrups (with a specified yielding strength of 785 MPa), and the specified compressive strengths of the concrete that is used herein are 70 and 100 MPa. The purpose of this work is to investigate flexural crack control with a view to ensure the serviceability and reparability of HSRC beam members.

The usefulness of the flexural crack control equations, recommended by ACI 318-14, fib Model Code (2010), AIJ (2010) and JSCE (2007), in ensuring the serviceability of HSRC beam members, is investigated in this work. Based on comparisons among various specifications and for reasons of convenience for engineers or designers, the provisions of ACI 318-14 are modified to control the width of flexural cracks in HSRC beam members. Additionally, AIJ (2010) recommends the allowable stress of main bars to ensure the reparability of HSRC beam members that are subjected to short-term loading. On the basis of AIJ (2010) with respect to reparability, this work investigates the experimental data to identify a ratio of the residual maximum flexural crack width to the maximum flexural crack width at the peak deformation angle n_{max}. To maintain the residual maximum flexural crack width $\leqq$ 0.4 mm to ensure reparability, this work uses the ratio n_{max} to determine the allowable stress of the main bars in HSRC beam members that are subjected to short-term loading.

2. References Related to the Flexural Crack Width Control

This section reviews the literature on controlling the flexural cracks of an RC beam member. With respect to control of the width of a flexural crack, ACI 318 adopts the model of Frosch (1999) to calculate this width if the plane remains a plane while the member is stressed; reinforcement strain is distributed uniformly; the strain of the concrete is negligible and the crack width increases linearly with the distance to the neutral axis in the tension zone, as shown in Fig. 1. The concrete crack width w_s in the reinforcing bar can be calculated as the product of the crack spacing S_c and the reinforcement strain ε_s (Eq. 1). To calculate the flexural

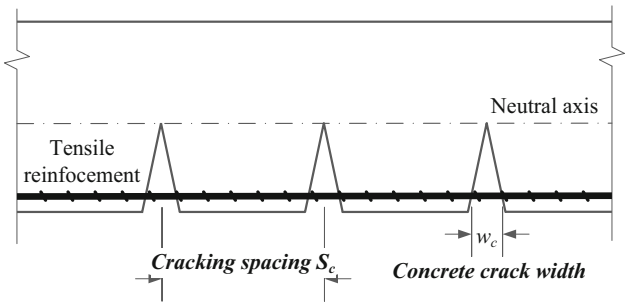

Fig. 1 Model of the flexural crack width in ACI 318.

crack width in the surface of the concrete w_c, the width of the crack in the width at the reinforcement w_s shall be multiplied by the strain gradient amplification coefficient β_s (Eq. 2). The reference (Frosch 1999) suggests using Eqs. (3) and (4) to evaluate the strain gradient amplification coefficient β_s (Fig. 2).

$$w_s = S_c \times \varepsilon_s \tag{1}$$

$$w_c = \beta_s \times S_c \times \varepsilon_s \tag{2}$$

$$\beta_s = \frac{\varepsilon_1}{\varepsilon_2} = \frac{h - x}{d - x} \tag{3}$$

$$\beta_s = 1.0 + 0.03 \times d_c \tag{4}$$

where h is the depth of a section (mm); d is the effective depth of a section (mm); x is the distance from the neural axis to the outmost compressive fiber of concrete (mm); d_c is the distance from the centroid of the outmost tensile reinforcement to the outmost tensile fiber of the concrete in the bottom surface (mm).

Since the design of an RC member for serviceability assumes that the stress of the reinforcement is in the linearly elastic range, Eq. (2) can be revised to Eq. (5), where f_s denotes the reinforcement stress under the service-level loading (MPa) and E_s is the elasticity modulus of reinforcement (MPa). Frosch (1999) showed that flexural crack spacing remains constant when the reinforcement stress reaches 140–210 MPa. Furthermore, the minimum crack spacing in the steady state almost equals the maximum distance from the outermost reinforcement centroid to the surface in the tension side (Eq. (6)). Frosch (1999) also pointed out that the average crack spacing and maximum crack spacing are 1.5 and 2 times the minimum crack spacing, respectively.

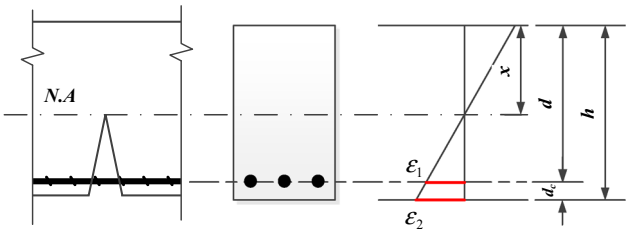

Fig. 2 Definition of the strain gradient amplification coefficient.

$$w_c = \beta_s \times S_c \times \frac{f_s}{E_s} \tag{5}$$

$$S_c = \psi_s \times d^* \tag{6}$$

$$d_1^* = \sqrt{d_c^2 + d_s^2} \tag{7}$$

$$d_2^* = \sqrt{d_c^2 + (\frac{s}{2})^2} \tag{8}$$

where ψ_s is the crack spacing factor; the minimum, average, and maximum crack spacing are 1.0, 1.5, and 2.0, respectively; d^* is the maximum distance from the centroid of the outermost tensile reinforcement to the outmost tensile fiber of the concrete (mm); d_s is the distance from the centroid of the outermost tensile reinforcement to the outmost tensile fiber of concrete in the side surface (mm); and d_1^* and d_2^* are defined as Eqs. (7) and (8) (Fig. 3).

Since ACI 318 assumes that d_1^* exceeds d_2^*, Eqs. (6) and (8) can be substituted into Eq. (5); then, Eq. (9) can be obtained to estimate the maximum flexural crack width. On the basis of Eqs. (9), (10) provides the original formula of the tensile reinforcement spacing, which can be used to control the flexural crack width. If the allowable maximum flexural crack width is set to 0.40 and 0.50 mm under the various tensile stresses of the reinforcement ($0.4f_y$ and $0.6f_y$), respectively, the corresponding curves for the limiting value of the reinforcement spacing considering can be obtained as shown in Fig. 4. For convenience, the distance from the center of the reinforcement to the concrete surface is replaced by the thickness of the concrete cover of the reinforcement C_c; then, the related design formulas of ACI 318-02 (2002) are obtained as Eqs. (11) and (12). In ACI 318-05, Eqs. (11) and (12) are replaced by Eqs. (13) and (14). If the reinforcement spacing is set equal to the limiting values of Eqs. (11) and (12) in ACI 318-05, then the maximum flexural crack width can be controlled within the range from 0.40 to 0.50 mm. ACI 318-14 also uses the design equations that were recommended by ACI 318-05 for flexural crack width control.

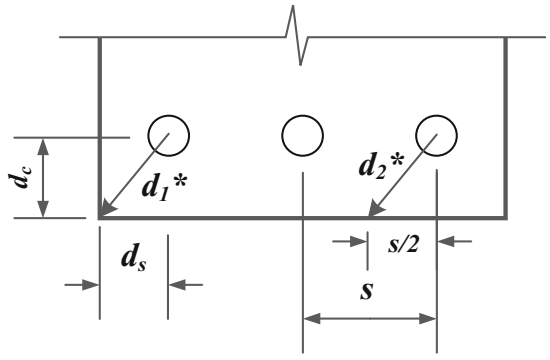

Fig. 3 Maximum distance from the outermost reinforcement centroid to the surface in the tension side.

$$w_{max} = 2\frac{f_s}{E_s}\beta_s\sqrt{d_c^2 + (\frac{s}{2})^2} \tag{9}$$

$$s = 2\sqrt{(\frac{w_{\max}E_s}{2f_s\beta_s})^2 - d_c^2} \tag{10}$$

$$s \le 380\frac{250}{f_s} - 2.5C_c \tag{11}$$

$$s \le \frac{300 \times 252}{f_s} \tag{12}$$

$$s \le 380\frac{280}{f_s} - 2.5C_c \tag{13}$$

$$s \le \frac{300 \times 280}{f_s} \tag{14}$$

In fib Model Code (2010), Eq. (15) is used to calculate the maximum flexural crack width in concrete close to the tensile reinforcement in an RC beam member. In Eq. (15), $l_{s,max}$, which can be estimated using Eq. (16), denotes the slip length between the concrete and reinforcement (mm). Clearly, the second item of Eq. (16) is derived from the equilibrium between the tensile force and the bonding force in the free body of concrete when an RC beam member is subjected to pure tension, as shown in Fig. 5. The term $(\varepsilon_{sm}-\varepsilon_{cm}-\varepsilon_{cs})$ in Eq. (15) represents the relative mean strain between the reinforcement and concrete, and it can be calculated using Eq. (17). For beam members subjected to a bending moment, the flexural crack width at the outmost tensile fiber of the concrete can be obtained from the flexural crack width in the concrete close to the tensile reinforcement multiplied by the strain gradient amplification coefficient β_s, as defined in Eqs. (3) or (4).

$$w_c = 2 \times l_{s,\max} \times (\varepsilon_{sm} - \varepsilon_{cm} - \varepsilon_{cs}) \tag{15}$$

$$l_{s,\max} = k \times c + \frac{1}{4} \times \frac{f_{ctm}}{\tau_{bms}} \times \frac{\phi_b}{\rho_{s,ef}} \tag{16}$$

where ε_{sm} is the average reinforcement strain over the length $l_{s,max}$; ε_{cm} is the average concrete strain over the length $l_{s,max}$; ε_{cs} is the strain of the concrete due to shrinkage; k is an empirical parameter to take the influence of the concrete cover into consideration ($k = 1.0$ can be assumed as a simplification); c is the thickness of the concrete cover (mm); and τ_{bm} is the mean bonding strength between the reinforcement and concrete (MPa).

$$\varepsilon_{sm} - \varepsilon_{cm} - \varepsilon_{cs} = \frac{\sigma_s - \beta \times \sigma_{sr}}{E_s} - \eta_r \times \varepsilon_{sh} \tag{17}$$

where σ_s is the reinforcement stress in a crack (MPa); σ_{sr} is the maximum reinforcement stress in a crack in the crack formation stage (MPa); $\rho_{s,ef}$ is defined as $A_s/A_{c,ef}$ (A_s is the total area of the tensile reinforcement (mm^2) and $A_{c,ef}$ is the effective area of the concrete in tension (mm^2)); β is an empirical coefficient to assess the mean strain over $l_{s,max}$

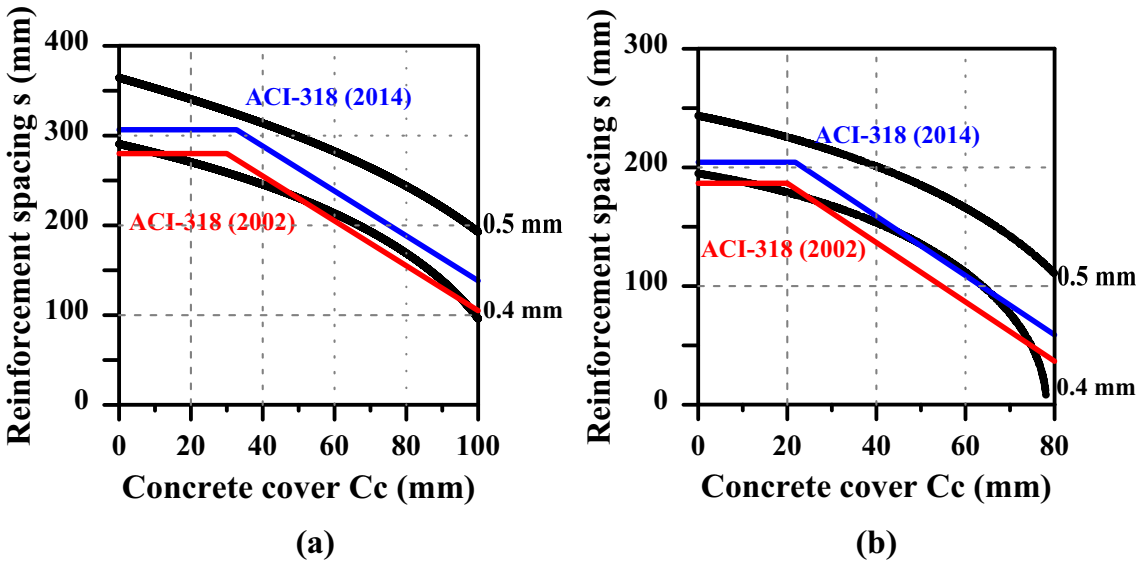

Fig. 4 Design equations in ACI 318-02 and ACI 318-14 for the flexural crack width control **a** $f_s = 0.4f_y$ and **b** $f_s = 0.6f_y$.

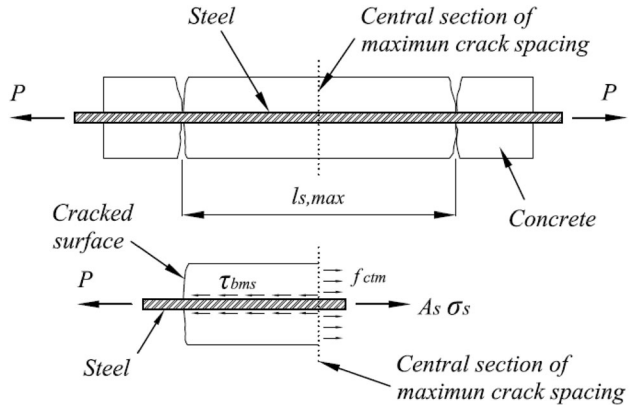

Fig. 5 Equilibrium between the tensile force and the bonding force in the free body of the concrete.

depending on the loading type; η_r is a coefficient for considering the shrinkage contribution; and ε_{sh} is the shrinkage strain.

For the purpose of controlling flexural cracks in an RC beam member, the Architectural Institute of Japan (AIJ; AIJ 2010) sets allowable stresses of the concrete and reinforcement under a long-term loading. Based on experimental data, the allowable stress allows a maximum crack width of 0.2–0.25 mm indoors and 0.3–0.4 mm outdoors. Equation (18) provided in the appendix of AIJ (2010) can be used to calculate the average flexural crack width of a beam or plate under a long-term load w_{av}. Since the average flexural crack width that is calculated using Eq. (18) is assumed to be in the concrete close to the tensile reinforcement, it can be used to calculate the average width of flexural cracks at the concrete surface by applying the strain gradient amplification coefficient β_s, as defined in Eqs. (3) or (4).

Along with average strain of tensile reinforcing bars $\varepsilon_{s,av}$ and the dry shrinkage of the concrete ε_{sh} (second term in Eq. 18), the thicknesses of the side and bottom concrete covers c_b (mm) and c_s (mm), the effective tensile reinforcement ratio p_e, the spacing of the tensile reinforcement s (mm), and the diameter of the tensile reinforcement ϕ_b(mm), are all included in the first item in Eq. (19), which yields average crack spacing l_{av} in Eq. (18) (mm). According to AIJ (2010), these equations are applicable to high-strength concrete with a compressive strength of 60–100 MPa. AIJ (2010) also recommends a maximum flexural crack width w_{max} of the average crack width multiplied by 1.5.

According to Zhao and Maruyama (2004), the first term in Eq. (19) is related to the distance from a crack surface to a concrete section that reaches the tensile strength of the concrete f_t. For a new crack surface in the concrete, the development length for the tensile strength uniformly distributed in a section is also required and can be estimated using the second term in Eq. (19). However, since Eqs. (20) and (21) shall be satisfied simultaneously to obtain the average strain of tensile reinforcing bars, engineers cannot easily calculate the maximum or average flexural crack width using AIJ (2010).

$$w_{av} = l_{av} \times \left(\varepsilon_{s,av} + \varepsilon_{sh}\right) \tag{18}$$

$$l_{av} = 2 \times \left(\frac{c_b + c_s}{2} + \frac{s}{10}\right) + 0.1\frac{\phi_b}{p_e} \tag{19}$$

$$\varepsilon_{s,av} = \frac{1}{E_s}\left(\sigma_s - K \times \frac{f_t}{\rho_e}\right) \tag{20}$$

$$K = \frac{1}{\left(2 \times 10^3 \times \varepsilon_{s,av} + 0.8\right)} \tag{21}$$

JSCE (2007), published by the Japan Society of Civil Engineering, adopts Eq. (18) to estimate the maximum flexural crack width on a concrete surface. The parameters in Eq. (22) include the type of reinforcement, the effective stress of the tensile reinforcement f_{se} (MPa), the thickness of the concrete cover c (mm), the spacing of the tensile reinforcement s (mm), the diameter of the tensile reinforcement ϕ_b(mm), the number of layers of the tensile reinforcement n and the compressive strength of concrete f_c' (MPa). JSCE

Table 1 HSRC Beam Specimens of the past researches (Chiu et al. 2014, 2016).

Spec.	N	C_c (mm)	S (cm)		f_y (MPa)	f_{yt} (MPa)	f'_c (MPa)	a/d	ρ_t (%)	ρ_s (%)	
			Left	Right						Left	Right
8H70	8	40	20	30	685	785	88.7	3.33	1.7	0.32	0.21
8H100	8	40	20	30	685	785	98.6	3.33	1.7	0.32	0.21
8N70	8	40	20	30	685	420	93.5	3.33	1.7	0.32	0.21
8N100	8	40	20	30	685	420	103.5	3.33	1.7	0.32	0.21
8NS100	8	40	Non-stirrup		685	–	105.1	3.33	1.7	–	
12H70	12	40	20	30	685	785	88.7	3.33	2.5	0.32	0.21
12H100	12	40	20	30	685	785	98.6	3.33	2.5	0.32	0.21
12N70	12	40	20	30	685	420	93.5	3.33	2.5	0.32	0.21
12N100	12	40	20	30	685	420	103.5	3.33	2.5	0.32	.021
12NS100	12	40	Non-stirrup		685	–	105.1	3.33	2.5	–	
6W70	6	40	20	30	685	785	73.7	3.33	2.02	0.32	0.21
6H70	6	40	20	30	685	785	70.7	3.33	2.02	0.32	0.21
175R70	6	40	30		685	785	87.9	1.75	3.5	0.24	
200R70	6	40	30		685	785	91.2	2	3.5	0.24	
275R70	6	40	30		685	785	76.8	2.75	3.5	0.24	
325R70	6	40	30		685	785	75.5	3.25	3.5	0.24	
175R100	6	40	30		685	785	90.4	1.75	3.5	0.24	
200R100	6	40	30		685	785	92.3	2	3.5	0.24	
275R100	6	40	30		685	785	83.1	2.75	3.5	0.24	
325R100	6	40	30		685	785	87.1	3.25	3.5	0.24	

N is the number of the tensile reinforcing bars, f_{yt} is the specified yielding stress of the transverse reinforcement, a/d is the ratio of the shear span to the effective depth of a section, ρ_t is the ratio of main bars, ρ_s is the ratio of the transverse reinforcement.

Table 2 HSRC beam specimens conducted in this work.

Spec.	N	C_c (mm)	S (cm)		f_y (MPa)	f_{yt} (MPa)	f'_c (MPa)	a/d	ρ_t (%)	ρ_s (%)	
			Left	Right						Left	Right
2C100	12	20	20	30	685	785	124.4	3.33	2.42	0.32	0.21
3C100	12	30	20	30	685	785	133	3.33	2.45	0.32	0.21
2C15S	6	20	15		685	785	99.9	3.5	1.94	0.42	
2C20T	6	20	20		685	785	101.9	3.5	1.94	0.41	
3C15S	6	30	15		685	785	87.4	3.5	1.98	0.42	
3C20T	6	30	20		685	785	90.9	3.5	1.98	0.41	
4C15S	6	40	15		685	785	95.4	3.5	2.01	0.42	
4C20T	6	40	20		685	785	89.4	3.5	2.01	0.41	
5C15S	6	50	15		685	785	84.6	3.5	2.04	0.41	

(2007) allows cracking in a general service state, but the width of the cracks may not exceed 0.3 mm.

$$w_{\max} = 1.1 \times k_1 k_2 k_3 \times [4c + 0.7(s - \phi_b)][\frac{f_{se}}{E_s} + \varepsilon'_{csd}] \quad (22)$$

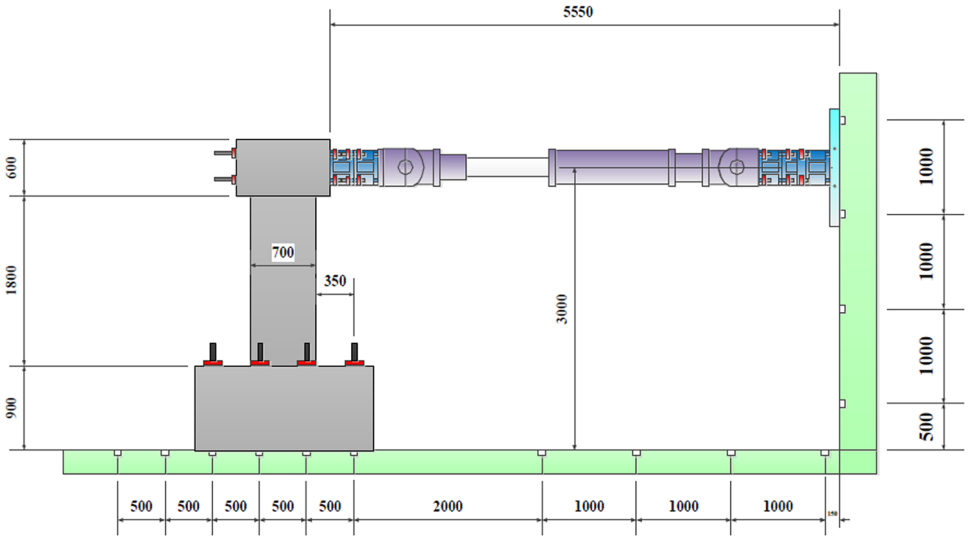

Fig. 6 Applied loading system for the cantilever beam specimens in this work (unit: mm).

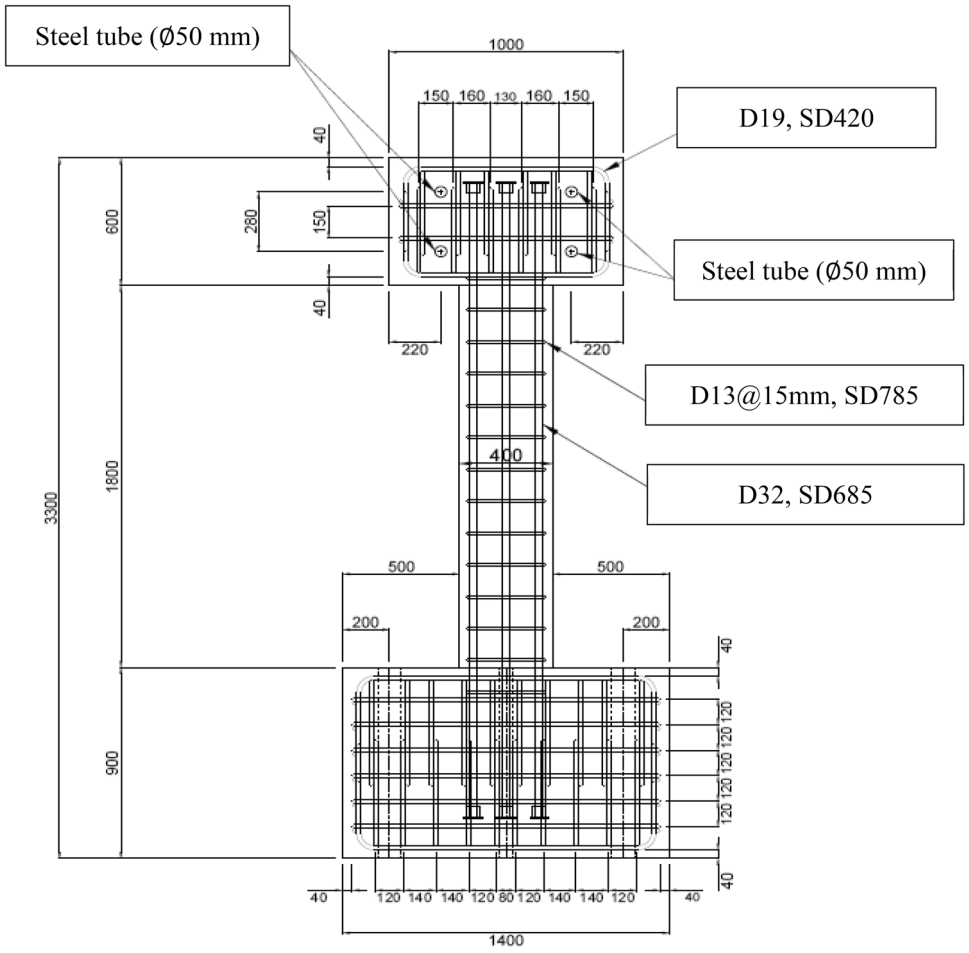

Fig. 7 Cantilever beam specimen of 3C15S (unit: mm).

Since the strength of bonding between the concrete and reinforcement influences the flexural crack width, JSCE (2007) uses parameters k_1 and k_2 to account for the effects of the surface geometry of the reinforcement and the strength of concrete on the bonding strength. The parameter k_1 is set at 1.0 for deformed bars and 1.3 for non-deformed bars or prestressed bars. Equation (23) for parameter k_2 indicates that stronger concrete is associated with a smaller maximum flexural crack width; however, k_2 cannot be less than 0.9. Equation (24) for parameter k_3 indicates that more layers of the tensile reinforcement are associated with a smaller maximum flexural crack width.

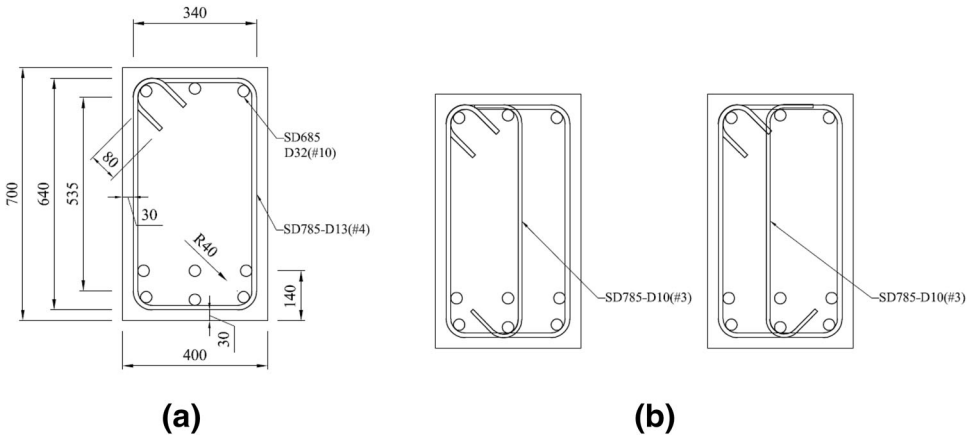

Fig. 8 Detailed reinforcement arrangement of the specimen sections. **a** 3C15S and **b** 3C20T.

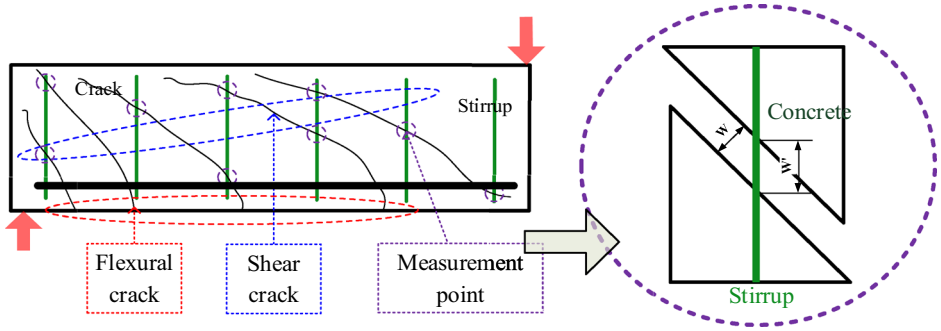

Fig. 9 Measuring cracks of various types at various positions in a specimen.

$$k_2 = \frac{15}{f_c' + 20} + 0.7 \tag{23}$$

$$k_3 = \frac{5(n+2)}{7n+8} \tag{24}$$

ε'_{csd} accounts for the effect of the concrete shrinkage and creep on the flexural crack width. Since ε'_{csd} is influenced by the shape of a member section, environmental conditions and stress, it must be determined with reference to various structural performance requirements, such as serviceability and durability. Based on the JIS testing method, the strain of concrete shrinkage and creep ε'_{csd} is 1000×10^{-6}; a value of $300–450 \times 10^{-6}$ is recommended if the age of the concrete is 30–200 days.

3. Experimental Setup and Results

This section describes the setup for testing HSRC beam specimens. Nine full-size beam specimens are tested to investigate the relationship between flexural crack development and deformation of the member. Some of the experiments that were conducted by Chiu et al. (2014, 2016) are also investigated in this work. All tests were performed at the National Center for Research on Earthquake Engineering, Taiwan (NCREE).

3.1 HSRC Beam Specimens Conducted in Previous Research (Chiu et al. 2014, 2016)

Chiu et al. (2014) designed ten simply-supported beam specimens to conduct the monotonic four-loading test, as indicated in Table 1. Applied lateral loading was controlled by varying the deformation at the mid-point of each specimen. The main bars were SD685 of D25, while the stirrups were SD420 and SD785 of D13. The equivalent shear regions on the right and left-hand sides of the beam specimens were designed with two stirrup spacings (200 and 300 mm). Each specimen was 6600 mm long, and the two equivalent shear regions and the equivalent moment region have the same span of 2000 mm in one specimen. The size of the section was 400 mm (width) × 700 mm (depth) and the thickness of concrete cover was 40 mm. Additionally, the measured compressive strength of the concrete was approximately 88.7–105.1 MPa.

Chiu et al. (2016) used ten simply-supported beam specimens and the loading system that was used in their earlier work (Chiu et al. 2014). The main bars were SD685 of D32, while the stirrups were SD785 of D13. The equivalent shear regions on the right and left-hand sides of the beam specimens were designed with the stirrup spacing of 300 mm. The length of the specimens was 6600, 4600 and 2600 mm, and the size of the section of the specimens was 350 mm (width) × 500 mm (depth) and 400 mm (width) × 700 mm (depth). Additionally, the shear span-to-depth ratios of the specimens were 3.33, 3.25, 2.75, 2.0 and 1.75. The

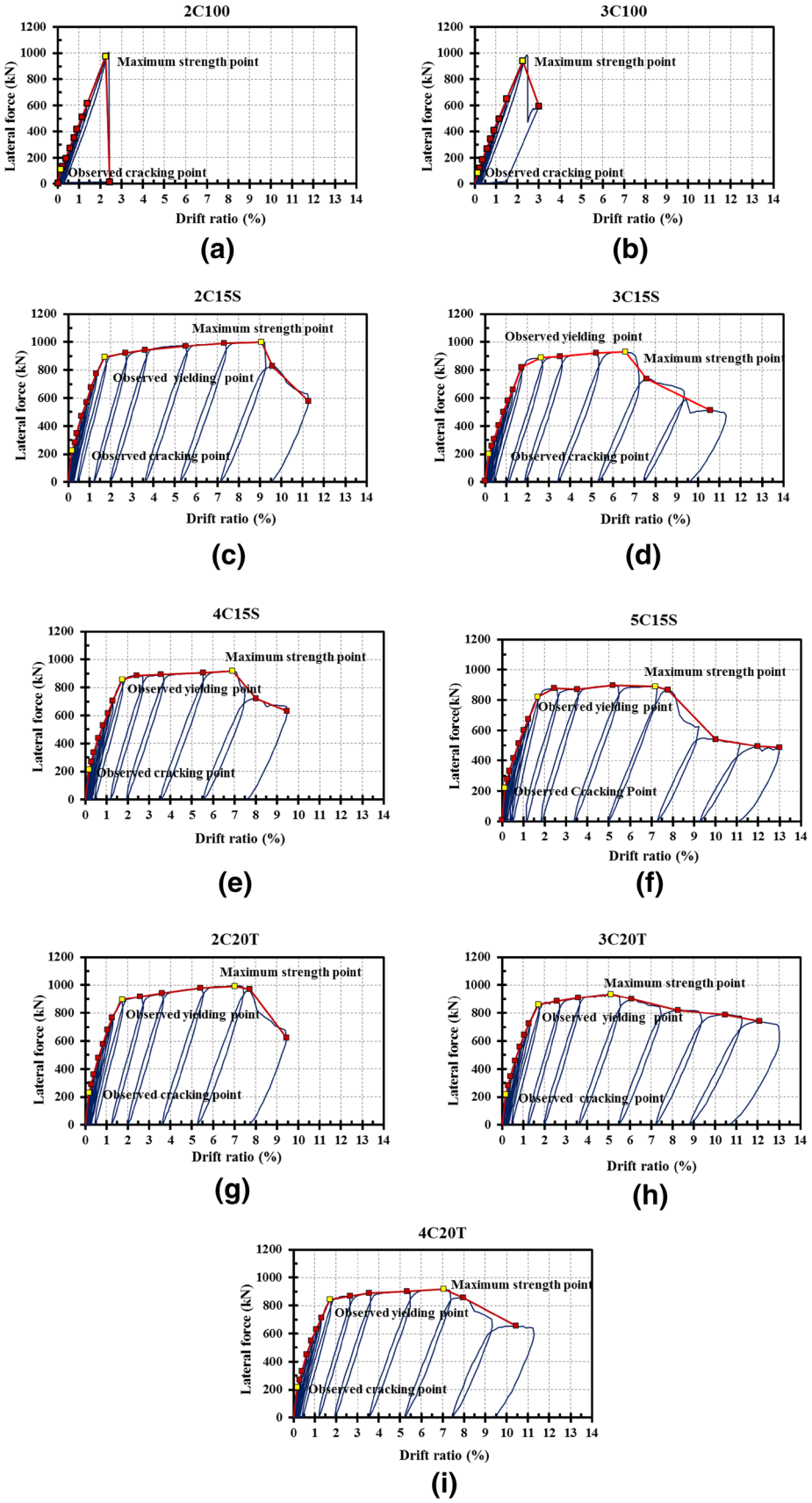

Fig. 10 Relationship between the lateral force and drift ratio of member for each specimen. **a** 2C100, **b** 3C100, **c** 2C15S, **d** 3C15S, **e** 4C15S, **f** 5C15S, **g** 2C20T, **h** 3C20T, and **i** 4C20T.

measured compressive strength of concrete was approximately 70.7–92.3 MPa.

In the symmetric monotonic loading test, the mechanical behavior of the equivalent shear region is similar to that of a beam member with a single curvature. It can also be

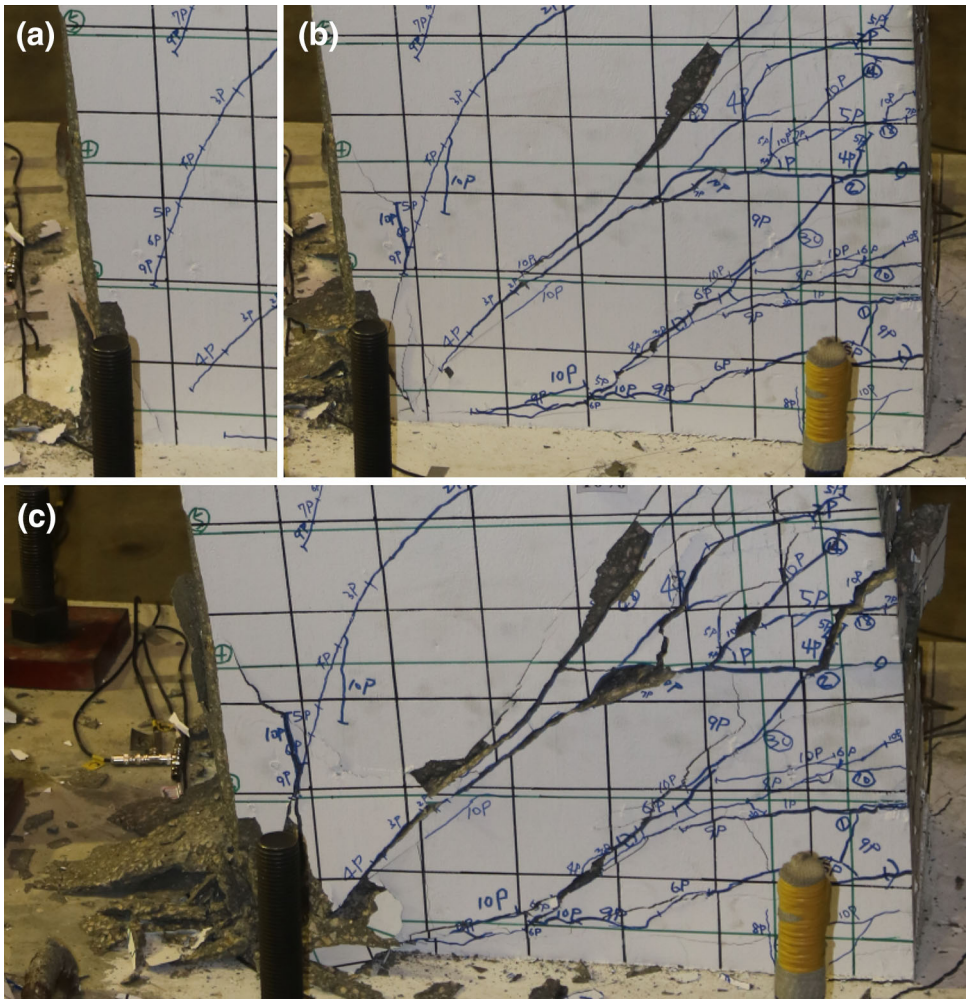

Fig. 11 **a** Concrete collapse on the compression side of the specimen (3%), **b** concrete cover spalling in the eastside of the specimen (6%), and **c** severe concrete collapse on the compression side of the specimen (10%).

assumed to be a half of the middle region of a beam member in the antisymmetric loading test based on the moment and shear distribution diagrams. Zakaria et al. (2009) used the symmetric monotonic loading method to investigate the shear crack behavior of RC beams with shear reinforcement. Therefore, Chiu et al. (2014, 2016) adopted the symmetric monotonic loading test to investigate shear crack behavior. For the 20 specimens listed in Table 1, the spacing of flexural cracks in the equivalent moment regions is investigated in this work. Additionally, some flexural-shear cracks in the equivalent shear regions are used to investigate the relationship between crack width and the stress of the reinforcement.

3.2 Experiment Setting

According to the reference in Sect. 2, the thickness of the concrete cover significantly influences the flexural crack width of concrete. Since the specimens that are listed in Table 1 have almost the same thickness as the concrete cover, 40 mm, seven cantilever beam specimens with the thicknesses of concrete cover of 20, 30, 40, and 50 mm, as listed in Table 2, are designed. Figure 6 shows the system for applying a load to the cantilever beam specimens. The loading system of Chiu et al. (2014) is also applied to two simply-supported beam specimens with two thicknesses of concrete cover, 20 and 30 mm. The two simply-supported beam specimens are of the same design and material as those used by Chiu et al. (2014).

The cantilever beam specimens herein are 1800 mm long and their cross-sections are 400 mm (width) × 700 mm (depth). Figure 7 shows the details of the specimen of 3C15S (Ho 2018). The main bars are SD685 of D32, while the stirrups are SD785 of D13. These specimens have the same tensile reinforcement ratio and stirrup ratio. Furthermore, two stirrup spacings of 150 and 200 mm are used to investigate the development of flexural cracks in specimens with a specified tensile reinforcement ratio and stirrup ratio. Two arrangements of the reinforcements in each specimen section includes are designed in this work, as shown in Fig. 8 (Ho 2018). The measured compressive strength of concrete is approximately 84.6–133 MPa.

To measure crack development, each specimen is brushed with white cement paint and 100 × 100 mm grid lines are drawn on it before testing. The actual stirrup position is marked on each specimen. The crack widths are measured using a microscope with a measurement resolution of 0.01 mm. The maximum crack width at a specified peak deformation and the residual crack width (with the applied

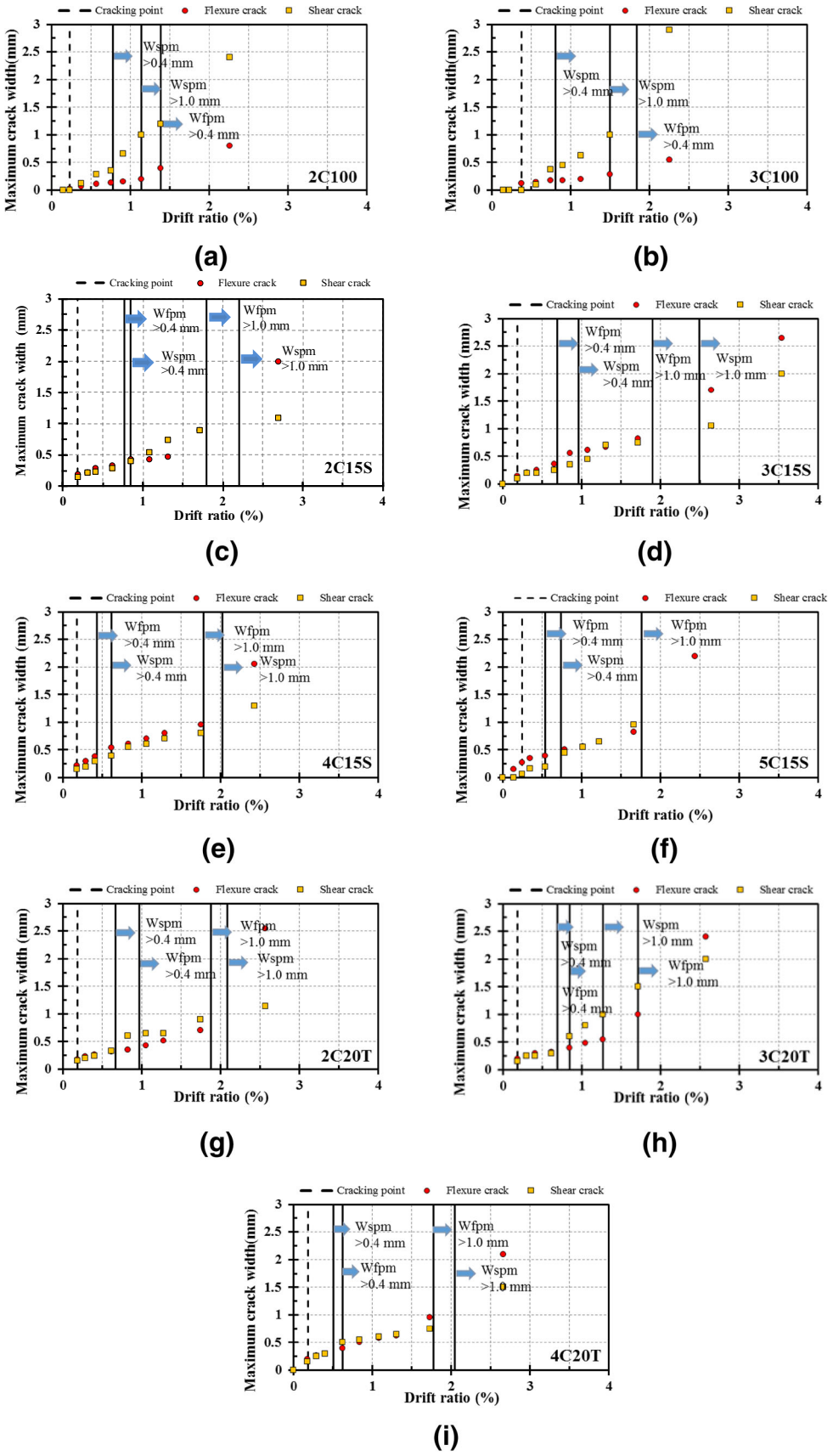

Fig. 12 Maximum crack width under various peak deformation angles. **a** 2C100, **b** 3C100, **c** 2C15S, **d** 3C15S, **e** 4C15S, **f** 5C15S, **g** 2C20T, **h** 3C20T, and **i** 4C20T.

loading set back to zero) at each measurement point are recorded in the experiment. The main purpose of the experiment is to measure flexural cracks. The methods for measuring cracks of various types at various positions are described as follows (Fig. 9):

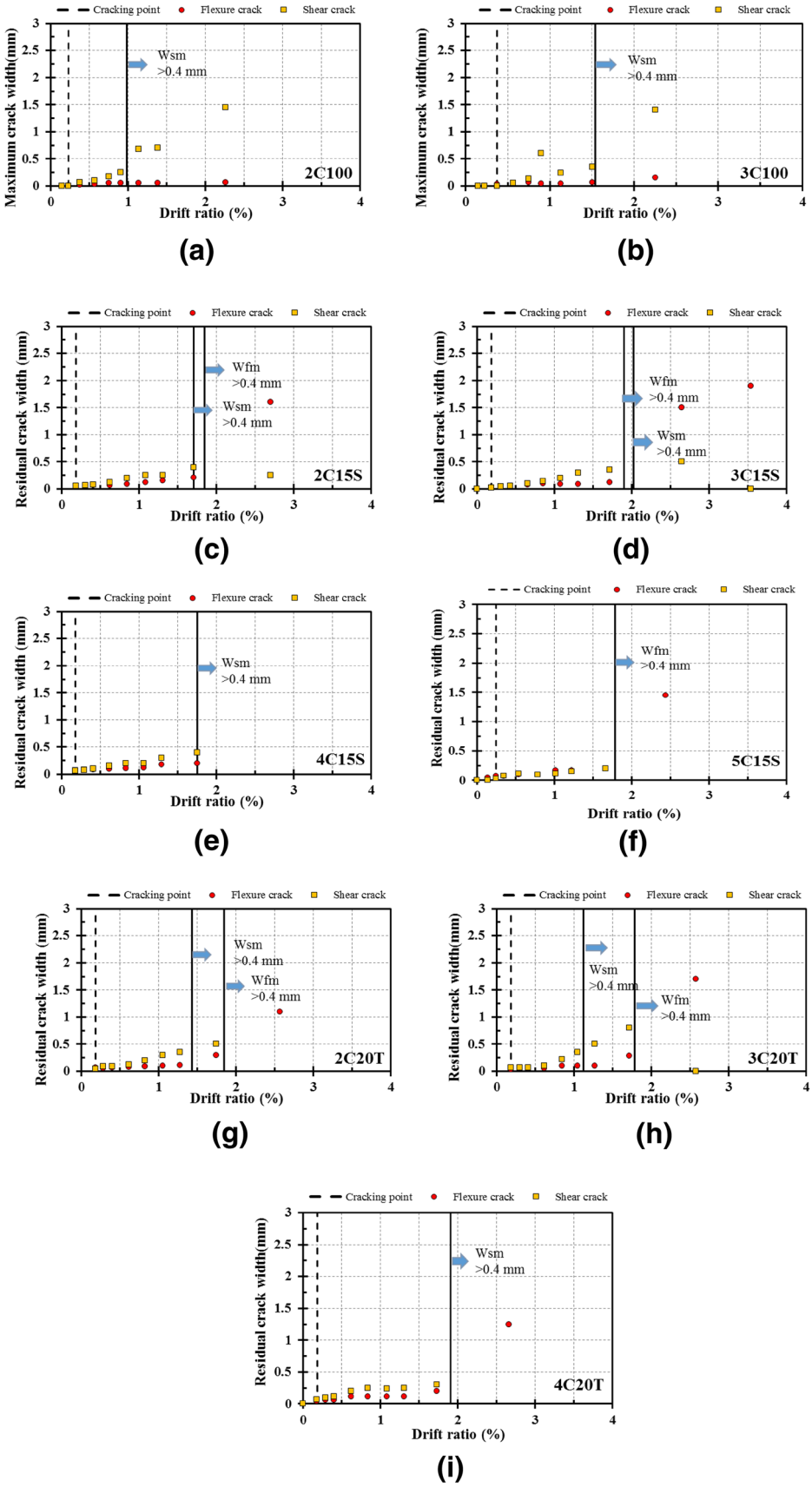

Fig. 13 Relationship between the residual maximum crack width and drift ratio of member at the peak deformation angle. **a** 2C100, **b** 3C100, **c** 2C15S, **d** 3C15S, **e** 4C15S, **f** 5C15S, **g** 2C20T, **h** 3C20T, and **i** 4C20T.

1. *Flexural crack* cracking occurs where the bending moment stress is at its maximum.
2. *Shear crack* cracking occurs where the shear stress is at its maximum. Furthermore, the width at the intersection between the shear crack and the stirrup, which includes

Table 3 Various specifications for the average flexural crack width.

Specifications	Average/maximum	Recommended equations
ACI-318 (2014)	Average spacing	$1.5\sqrt{d_c^2 + \left(\frac{s}{2}\right)^2}$
AIJ (2010)	Average spacing	$2\left(\frac{c_b+c_s}{2} + \frac{s}{10}\right) + 0.1\frac{\phi_b}{p_e}$
JSCE (2007)	Maximum spacing	$1.1k_1k_2k_3[4c + 0.7(s - \phi_b)]$
CEB-fib Model Code (2010)	Maximum spacing	$2 \times \left(k \times c + \frac{1}{4} \times \frac{f_{ctm}}{\tau_{bms}} \times \frac{\phi_b}{\rho_{s,ef}}\right)$

the shear crack width and the width parallel to the stirrup, is measured.

3.3 Experimental Results

In this work, two four-point loading simply-supported beam tests and seven cantilever beam tests are conducted. In the experiment herein, the development of the shear and flexural cracks is observed at various peak deformations angle of each specimen. When the applied loading is set back to be zero at a peak deformation angle, the residual shear and flexural crack widths are also measured.

Figure 10 plots the relationship between the lateral force and drift ratio of a member in each specimen that is tested in this work. For each specimen, the observed cracking point, measured yielding point and measured maximum strength point are indicated. As well as the relationship between the lateral force and the drift ratio of a member, the crack development and failure pattern of a member are also recorded in the experiment. Taking the specimen of 3C15S for an example, at a deformation angle of 0.25%, a shear crack is observed. At a deformation angle of 1.5%, the specimen exhibits a vertical crack along the main bars. At a deformation angle of 2%, the specimen has many vertical cracks, which are connected with the previously formed vertical crack in the specimen. The concrete collapses on the compressed side of the specimen at a deformation angle of 3% (Fig. 11a) and concrete cover spalling occurs at a deformation angle of 6% (Fig. 11b). For the maximum strength of the specimen, the lateral force of 929.5 kN is recorded at a deformation angle of 8%. After the maximum strength point of the specimen, the specimen exhibits serious damage along the primary shear crack in its eastside and severe concrete collapse occurs on the compressed side of the specimen (Fig. 11c); then, the strength decreases to 737.6 kN (79.35% of the maximum strength). Additionally, in the final step of a deformation angle of 12%, the strength is only 510.2 kN (54.8% of the maximum strength). Since this strength is less than 60% of the maximum strength, the experiment is stopped.

The method for measuring the width of cracks that was described in Sect. 3.2 is used to follow the width of the crack. Figure 12 plots the development of the maximum crack width at various peak deformation angles. The figure shows both the shear and flexural crack width and the observed cracking point. Figure 13 plots the relationship between the residual maximum crack width and the drift ratio of a member at a peak deformation angle. At a peak deformation angle in the experiment, it can be found that the shear crack width is larger than the flexural crack width for the specimens with the stirrup spacing $\geqq$20 mm. For the residual maximum crack width, the shear crack width is not smaller than the flexural crack width in this experiment. Furthermore, it can be found that the residual maximum flexural crack width increases to be close to the residual maximum shear crack width when the thickness of the concrete cover increasing (Fig. 13).

4. Flexural Crack Control for HSRC Beam Members

4.1 Flexural Crack Spacing

The equations, recommended in various specifications, for calculating the flexural crack width (Sect. 2) involve terms that can be divided into two groups—those that concern the difference between the strains of concrete and reinforcement, and those that concern the flexural crack spacing (Table 3). For the simply-supported beam specimens in this work, the average flexural crack spacing is calculated by dividing the equivalent moment segment lengths of various specimens by the number of cracks. For the cantilever beam specimens, the average flexural crack spacing in the development region of the plastic hinge is observed. Figure 14 plots the relationship between the average flexural crack spacing and the curvature or drift ratio of a member. Clearly, as the curvature or drift ratio of a member increases, the average spacing decreases and eventually becomes constant. Furthermore, in the experiment herein, the flexural crack width is proportional to the stress of reinforcing bars after the average crack spacing has become stable.

Figure 15 compares the measured average flexural crack spacing with the values calculated using various specifications (Table 3). According to Fig. 15, the average crack spacings that are calculated using various specifications are more conservative than the experimental values. Furthermore, according to Frosch (1999), ACI 318 requires that larger of the values of d_1^* and d_2^* shall be used to calculate the crack spacing (Eq. (6)). Table 4 lists the required parameters in Eq. (6) for each selected specimen. However, since d_2^* is identified as a main control item in Eq. (9), which is used in ACI 318 from 2002, the values for some specimens fall in the non-conservative region. Therefore, in this work, the average flexural crack spacing is calculated for all specimens

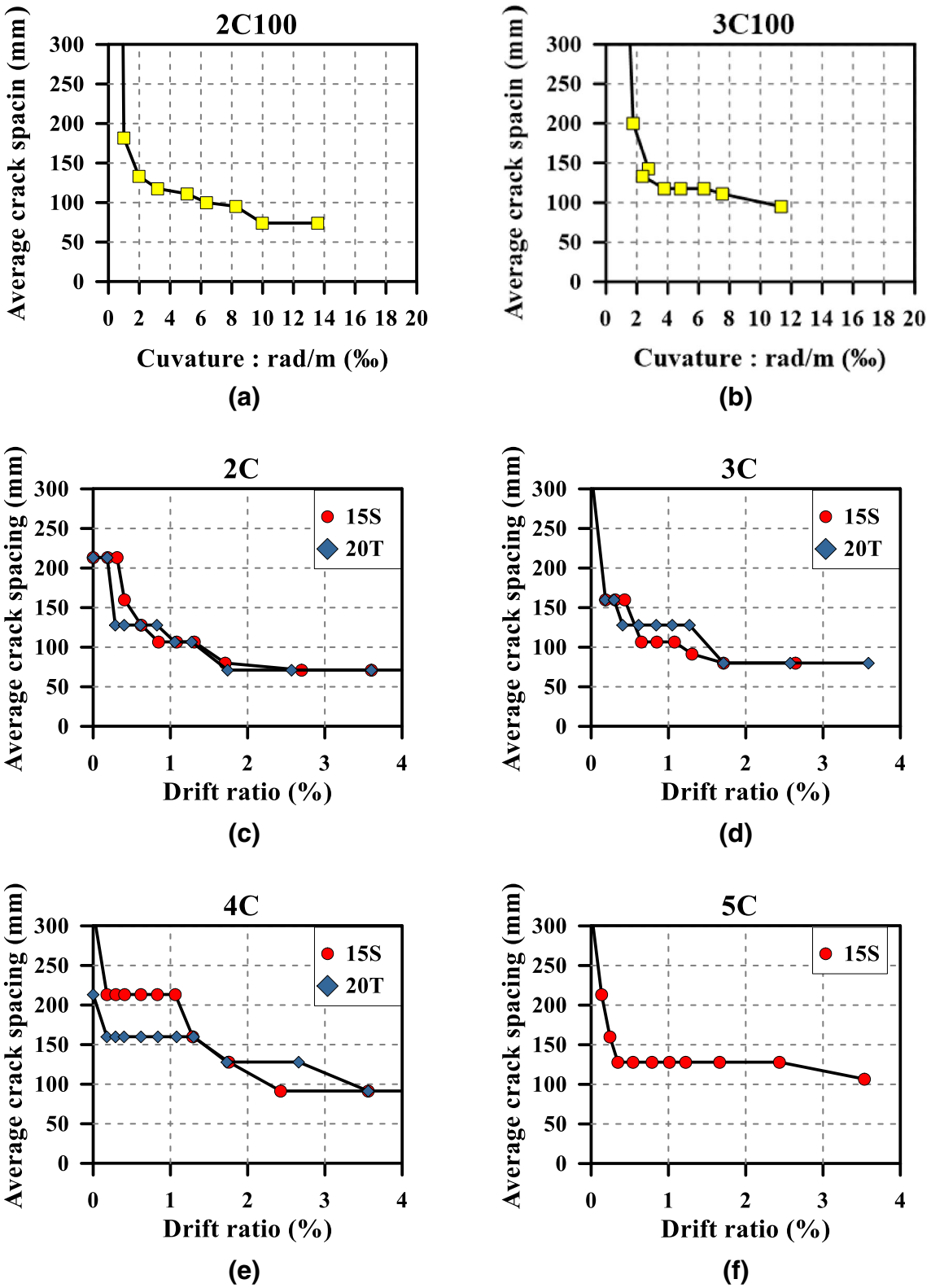

Fig. 14 Relationship between the average flexural crack spacing and curvature or drift ratio of member. **a** 2C100, **b** 3C100, **c** 2C15S and 2C20T, **d** 3C15S and 3C20T, **e** 4C15S and 4C20T, and **f** 5C15S.

on the basis of the larger of d_1^* and d_2^*, as shown in Fig. 16; then, all of the results are in the conservative region. Unlike those in AIJ (2010) and fib Model Code (2010), the equations that are recommended by ACI 318 and JSCE (2007) for the average flexural crack spacing are convenient for use by engineers or designers to control the width of cracks in HSRC beam members. Additionally, on the basis of the limited experimental data in this work, the average crack spacing can be predicted conservatively only using the concrete cover thickness and tensile reinforcement spacing, as shown in Fig. 16.

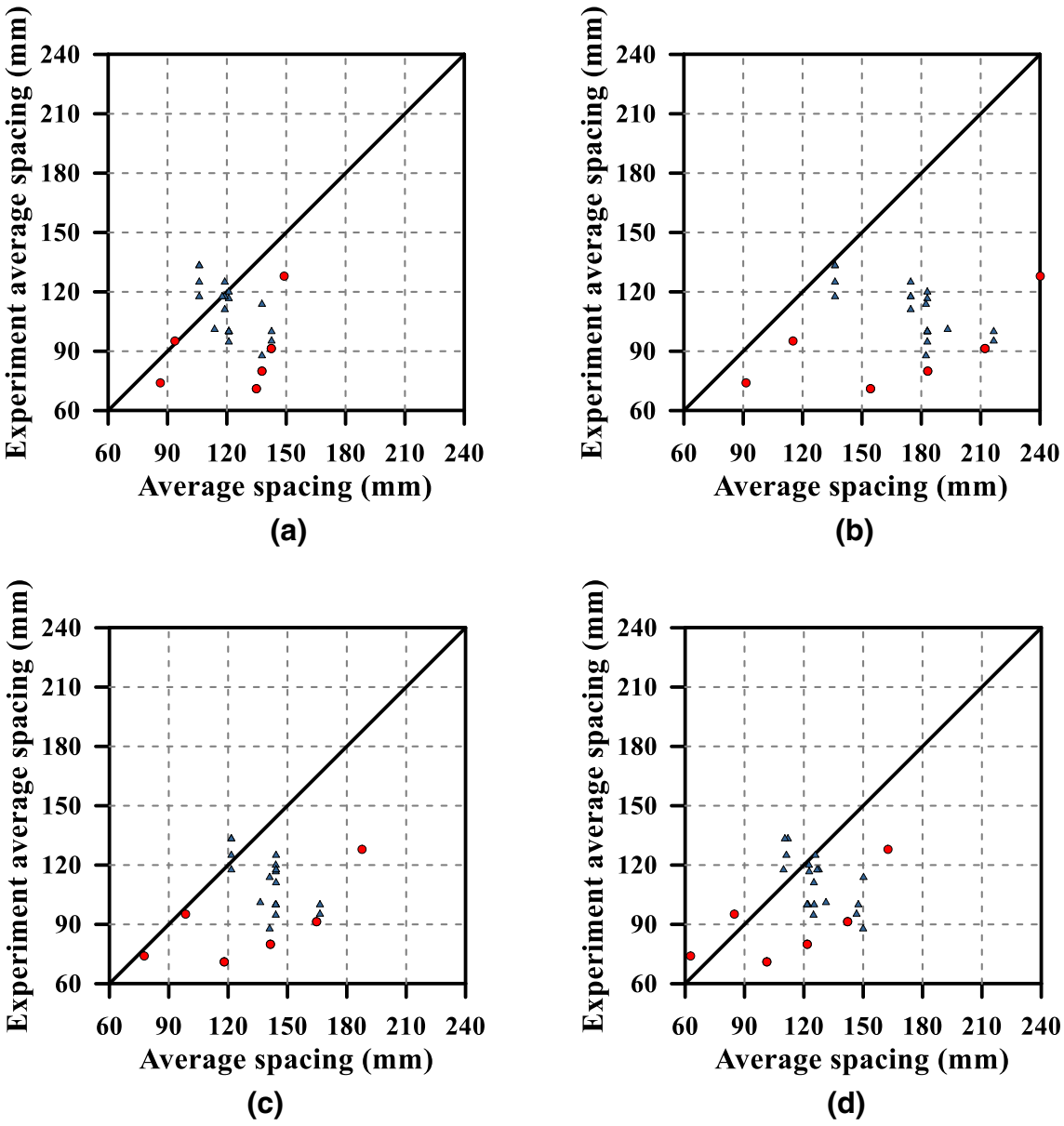

Fig. 15 Comparison of the experimental results and calculated values using various specifications for the average flexural crack spacing. **a** ACI 318 (2014), **b** CEB-fib Model (2010), **c** AIJ (2010), and **d** JSCE (2007) (Circle points are the specimens in this work; triangle points are the specimens in the references (Chiu et al. 2014, 2016)).

4.2 Flexural Crack Width

Figure 17 compares the measured maximum flexural crack width with the values calculated using various specifications. In this work, the shrinkage or creep strains of concrete in the selected specifications are not considered. Clearly, when the maximum flexural crack width is less than 1.0 mm, it can be predicted using the selected specifications. Furthermore, with respect to ACI 318 (Eq. (5)), when the maximum flexural crack spacing in all specimens is calculated using the larger value of d_1^* and d_2^*, those calculated values are more conservative than those calculated using only d_2^*, as shown in Fig. 17e. Additionally, Fig. 17e shows that Eq. (5) can predict the maximum flexural crack width conservatively when the calculated value is smaller than 0.8 mm.

This section also compares the calculated values of the maximum flexural crack width with the measured values under various stress ratios of the tensile reinforcement, f_s/f_y, as shown in Fig. 18. The comparison reveals that the equations for the maximum flexural crack width that are recommended by the specifications except for AIJ (2010) cannot provide conservative predictions. Furthermore, since the flexural crack spacing is not yet stable with low stress ratios of the tensile reinforcement, the calculated values of the maximum flexural crack width are much less than the measured values. Clearly, the equations for the maximum flexural crack width that are recommended by various specifications become more conservative as the stress ratio of the tensile reinforcement increases. Based on the comparisons among various specifications and for the convenience of engineers or designers, in this work, Eq. (9) that is recommended in ACI 318 is modified for control of the width of flexural cracks for HSRC beam members.

Table 4 Required parameters in Eq. (6).

Spec.	Required parameters in Eq. (6)			
	d_c (mm)	s (mm)	d_1^* (mm)	d_2^* (mm)
2C100	45.4	61.84	64.2	71.3
3C100	55.4	57.84	78.3	62.5
2C15S	48.6	151.425	68.7	90.0
2C20T	48.6	151.425	68.7	90.0
3C15S	58.6	141.425	82.8	91.8
3C20T	58.6	141.425	82.8	91.8
4C15S	68.6	131.425	97.0	95.0
4C20T	68.6	131.425	97.0	95.0
5C15S	78.6	121.425	111.1	99.3
8H70	65.37	89.753	92.5	79.29
8H100	65.37	89.753	92.5	79.29
8N70	65.37	89.753	92.5	79.29
8N100	65.37	89.753	92.5	79.29
8NS100	65.37	89.753	92.5	79.29
12H70	65.37	53.852	92.5	70.7
12H100	65.37	53.852	92.5	70.7
12N70	65.37	53.852	92.5	70.7
12N100	65.37	53.852	92.5	70.7
12NS100	65.37	53.852	92.5	70.7
6W70	68.8	131.2	97.3	95.1
6H70	68.8	131.2	97.3	95.1
175R70	68.8	84.2	97.3	80.7
200R70	68.8	84.2	97.3	80.7
275R70	68.8	84.2	97.3	80.7
325R70	68.8	84.2	97.3	80.7
175R100	68.8	84.2	97.3	80.7
200R100	68.8	84.2	97.3	80.7
275R100	68.8	84.2	97.3	80.7
325R100	68.8	84.2	97.3	80.7

$$\phi = 3 - 5\left(\frac{f_s}{f_y}\right), 0 \le \frac{f_s}{f_y} \le 0.4 \tag{25}$$

$$w_{max} = \phi \times \left(2\frac{f_s}{E_s}\beta_s\right) \times \left(\max\left(d_1^*, d_2^*\right)\right) \tag{26}$$

With respect to Eq. (5), this work takes $0.4f_y$ as the boundary on the steel stress and introduces a correction coefficient ϕ, given by Eq. (25), in the low-stress stage to increase the flexural crack spacing. Equation (5) is used and modified equation for the maximum flexural crack width, Eq. (26), is thus proposed. When Eq. (26) is used to calculate the maximum flexural width for all specimens, the average ratio of the measured maximum flexural crack width to the calculated maximum flexural crack width is 0.74, as shown in Fig. 19a. Therefore, Eq. (26) can predict the maximum flexural width conservatively.

4.3 Flexural Crack Control for HSRC Beam Members

According to Fig. 18, for HSRC beam specimens, the maximum flexural crack width can still be controlled well in the way recommended by ACI 318. However, in order to solve the non-conservative phenomenon under the low stress and not to change the pattern of the original equation (Eq. 9), a

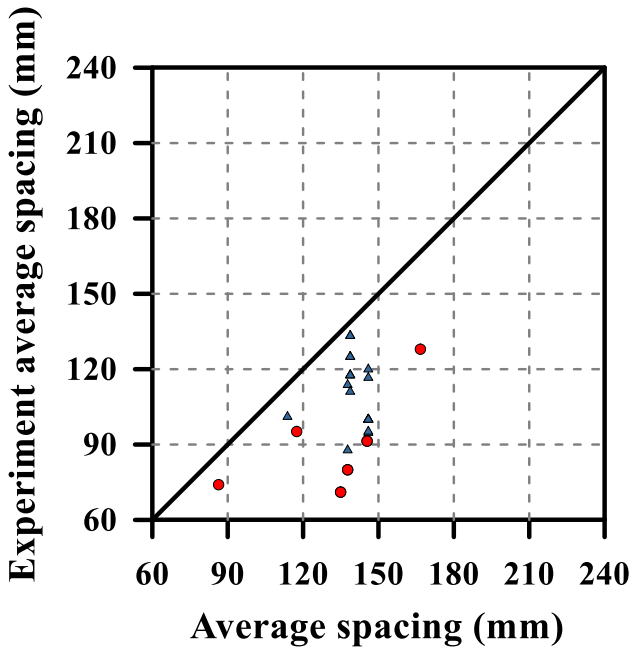

Fig. 16 Average flexural crack spacing calculated using Eq. (6) (Circle points are the specimens in this work; triangle points are the specimens in the references (Chiu et al. 2014, 2016)).

correction coefficient should be introduced in the stress ratio of the tensile reinforcement, as ($\phi \times (f_s/f_y)$). Restated, the non-conservative maximum flexural crack width in the low stress state can be solved by the constraint of the stress of the tensile reinforcement. According to the experimental results, the stress ratio of the tensile reinforcement considering the correction coefficient ϕ is in the range of 0.0–0.45. This work suggests the modified stress ratio of the tensile reinforcement is 0.4 based on its mean value of 0.36. As shown in Fig. 19e, if $f_s = 0.4fy$ is used instead of Eq. (25) when $f_s < f_y$ in Eq. (26), the average ratio of the measured to the calculated maximum flexural crack width using Eq. (26) is 0.72. Therefore, engineers or designers can calculate the maximum flexural crack width of a HSRC beam under the service loading according to ACI 318 (Eq. (26)). Additionally, if the calculated stress of the tensile reinforcement is lower than $0.4f_y$, then $0.4f_y$ shall be substituted in Eq. (26).

When the stress of the tensile reinforcement is $0.4f_y$ and $0.6f_y$, respectively, as shown in Fig. 4, the design equations recommended by ACI 318-02 can let the maximum flexural crack width smaller than 0.4 mm. Additionally, if the design equations recommended by ACI 318-14 (2014) are adopted, the maximum flexural crack width can be in the range of 0.4–0.5 mm. According to the investigation in Sect. 4.2, this work suggests the design equations of ACI 318-14 for controlling the flexural crack width under the service loading can be applied on HSCR beam members. Additionally, the minimum value of f_s is set at $0.4f_y$. However, according to Sect. 2, the design equations of ACI 318-14 are derived based on the assumption of $s \geqq 2d_c$; therefore, the allowable values of s are remarked as Zone I in Fig. 20.

If s is smaller than $2d_c$, Eq. (26) can be used to derive a maximum value of d_c for controlling the maximum flexural crack width as Eq. (27). Taking the maximum flexural crack width of 0.4 mm for an example, when the stress of the tensile reinforcement is $0.4f_y$ and, the maximum value of d_c is 105 mm calculated using Eq. (27). Additionally, Fig. 20 shows the allowable values of s remarked as Zone II for $s < 2d_c$. Therefore, for the maximum flexural crack width of 0.4 mm, Zone I and Zone II remarked in Fig. 20 are the allowable design region of s when the stress of the tensile reinforcement is set at $0.4f_y$ or $0.6f_y$.

Based on ACI 318-14, this work proposes the following equations (Eqs. (27), (28)) to do the flexural crack control for HSRC beam members. Additionally, when the maximum flexural crack width is set in the range of 0.4–0.5 mm as ACI 318-14, Eq. (27) can be approximated by Eq. (29) for a maximum value of d_c, as shown in Fig. 21 when $s \leqq 2d_c$.

$$d_c \leq \sqrt{\frac{w_{\max} E_s}{\sqrt{2} f_s} \times \left(\frac{1270}{4}\right) + \left(\frac{1270}{8}\right)^2} - \frac{1270}{8} \tag{27}$$

$$s \leq \max\left\{\min\left[380\frac{280}{f_s} - 2.5d_c, \frac{300 \times 280}{f_s}\right], 2d_c\right\} \tag{28}$$

$$d_c \leq 192 - 124 \times \left(\frac{f_s}{f_y}\right) \tag{29}$$

To ensure the reparability of an HSRC beam member in a medium-magnitude earthquake, the residual maximum flexural crack width of a member following an earthquake does not exceed 0.4 mm based on the reference. However, it is difficult to develop the relationship between the residual maximum flexural crack with and tensile stress of main bars based on the mechanical behaviors of RC members. Therefore, this work uses the experimental data to suggest the allowable stress of main bars to ensure the reparability of an HSRC beam member.

The allowable stress of the tensile reinforcement that guarantees the repair performance can be suggested based on the assumption that the residual maximum flexural crack width of a member following an earthquake does not exceed 0.4 mm. However, since it is not easy to unload the force to be the long-term loading in the experiment, the allowable stresses of the tensile reinforcement that ensure reparability cannot be directly determined. To identify the allowable tensile stress corresponding to the residual maximum flexural crack width of a member, a ratio between the maximum flexural crack width at the peak deformation angle and residual maximum flexural crack width, n_{max}, should be investigated in the experiment. According to the experimental results, there is no apparent linear relation between n_{max} and the deformation angle of a member (Fig. 22). Since the average value minus one standard deviation of n_{max} is 2.23, this work suggests n_{max} is 2.0 to calculate the maximum flexural crack width at the peak deformation angle. When the residual maximum flexural crack width is set at 0.4 mm, the allowable value of the maximum flexural crack width at the peak deformation angle is 0.8 mm. However, according to the relationship between the maximum flexural crack width and maximum stress of the tensile reinforcement

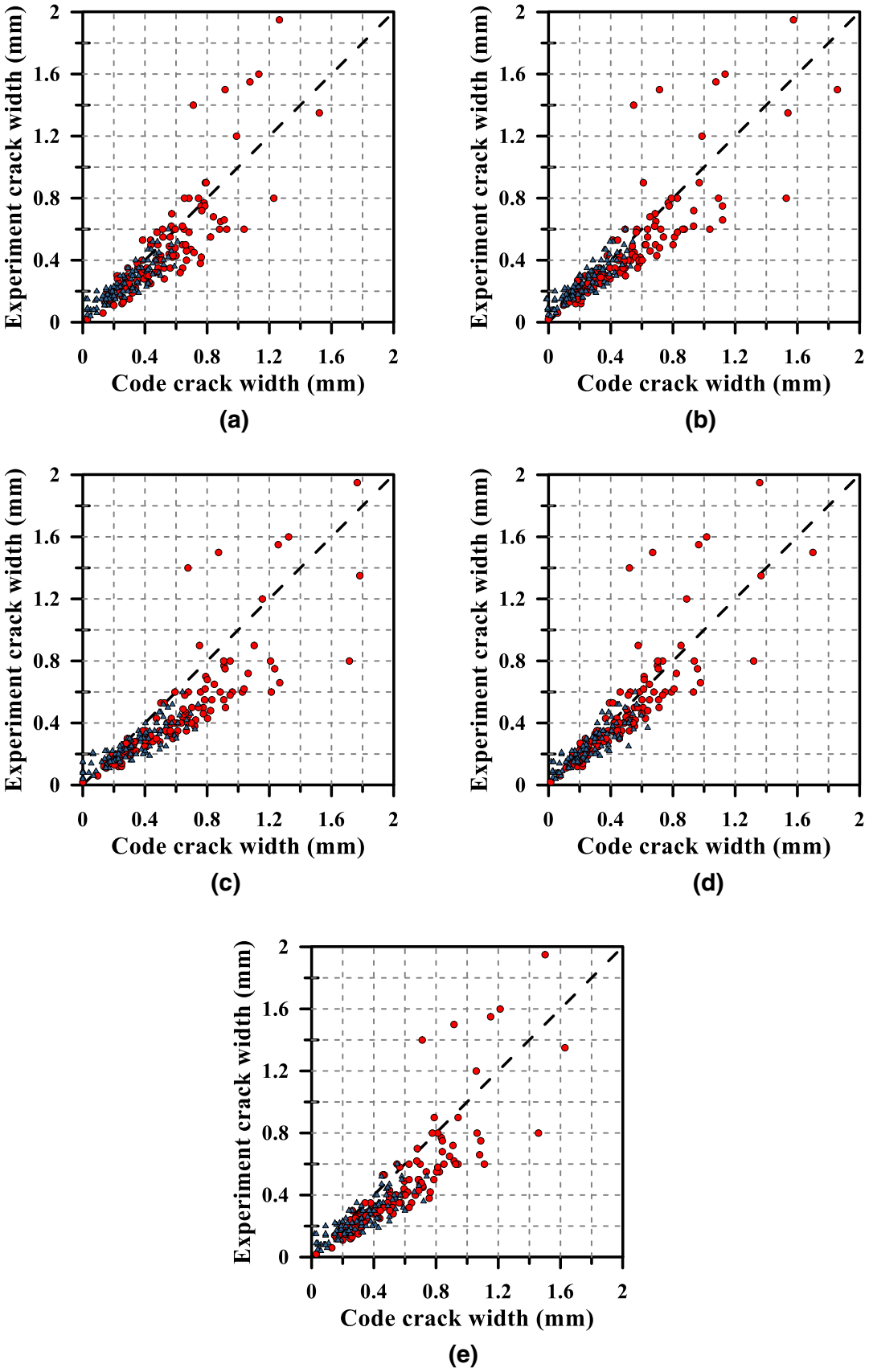

Fig. 17 Comparison of the measured and calculated maximum flexural crack widths. **a** ACI 318 (2014), **b** CEB-fib Model (2010), **c** AIJ (2010), **d** JSCE (2007), and **e** ACI 318 (2014) (Modified) (Circle points are the specimens in this work; triangle points are the specimens in the references (Chiu et al. 2014, 2016)).

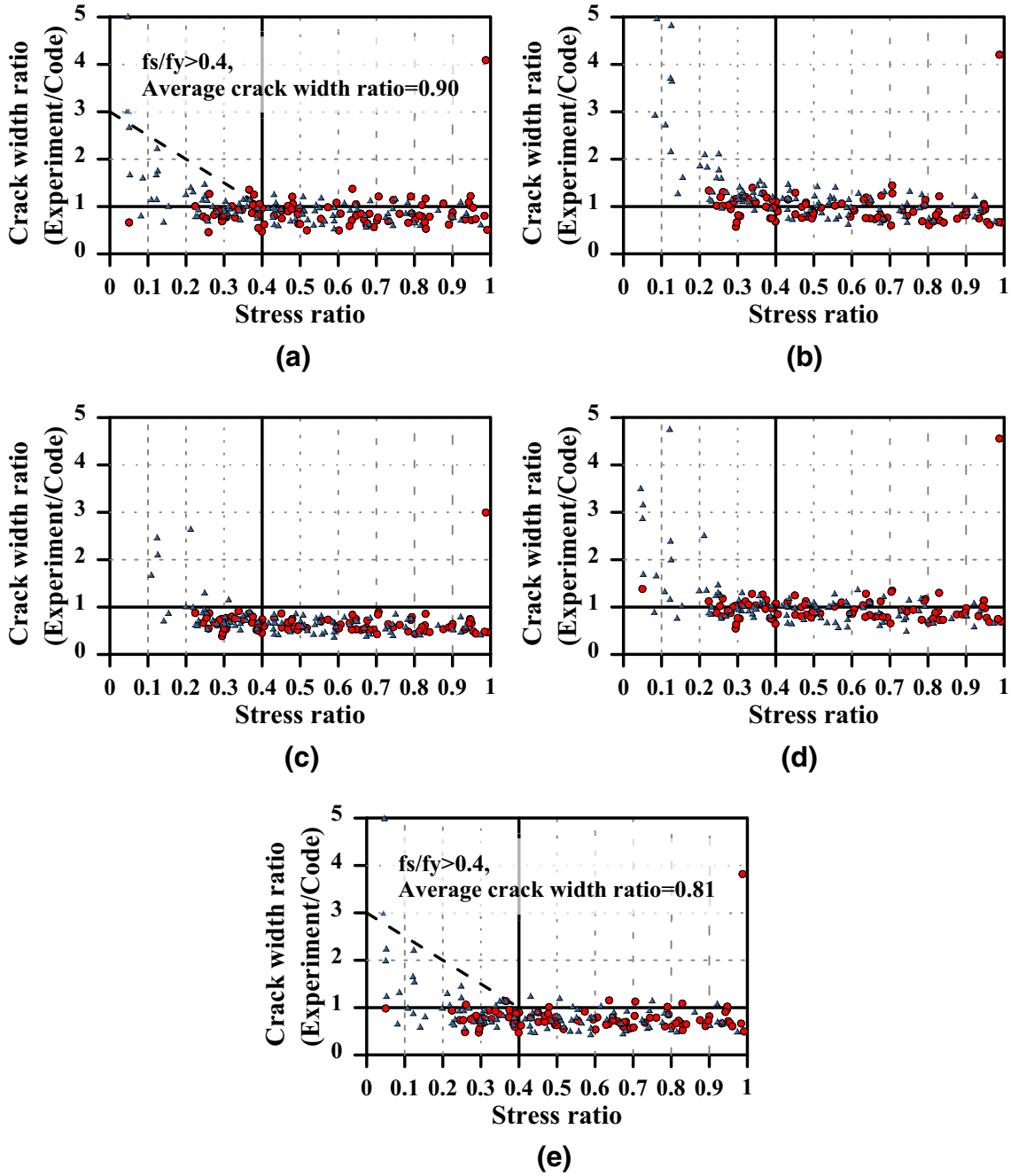

Fig. 18 Ratio of the measured and calculated maximum flexural crack widths under various stress ratios of the tensile reinforcement. **a** ACI 318 (2014), **b** CEB-fib (2010), **c** AIJ (2010), **d** JSCE (2007), and **e** ACI 318 (2014) (Modified) (Circle points are the specimens in this work; triangle points are the specimens in the references (Chiu et al. 2014, 2016)).

(Fig. 22), the maximum stress of the tensile reinforcement reaches the yielding stress before the maximum flexural crack width exceeds 0.8 mm. Therefore, to ensure the reparability of an HSRC beam member in a medium-magnitude earthquake, the allowable stress of tensile reinforcement can be set as the specified yielding stress of 685 MPa.

5. Conclusions

In this work, nine full-size HSRC beam specimens are utilized to investigate the relationship between flexural crack development and deformation. Some HSRC experiment data collected from Chiu et al. (2014, 2016) are also investigated. Experimental results are compared with various specifications that are related to flexural crack width control and modified equations for ACI 318-14 related to flexural crack width control are suggested. Designers or engineers can adopt the proposed equations (Eqs. (28), (29)) to design the spacing of tensile 1reinforcements or the thickness of the concrete cover, to control the flexural crack width of an HSCR beam member under service-level loading. Additionally, the minimal calculated stress of the tensile reinforcement in the proposed equations is $0.4f_y$.

According to the experimental data, when the residual maximum flexural crack width is limited to 0.4 mm, the allowable maximum flexural crack width at the peak deformation angle is 0.8 mm. According to the relationship

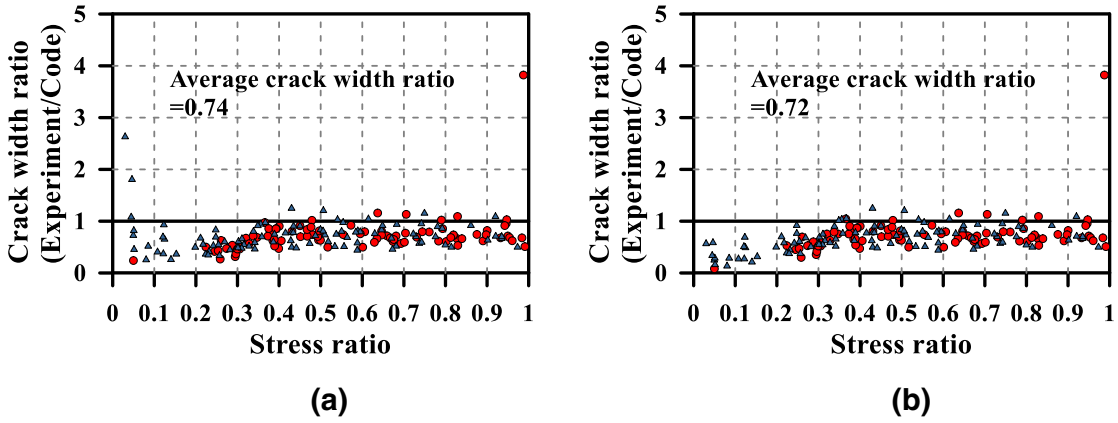

Fig. 19 Ratio of the measured and calculated maximum flexural crack widths using Eq. (26). **a** Using Eq. (25) and **b** Using $f_s = 0.4fy$ when $f_s < f_y$ instead of Eq. (25) (Circle points are the specimens in this work; triangle points are the specimens in the references (Chiu et al. 2014, 2016)).

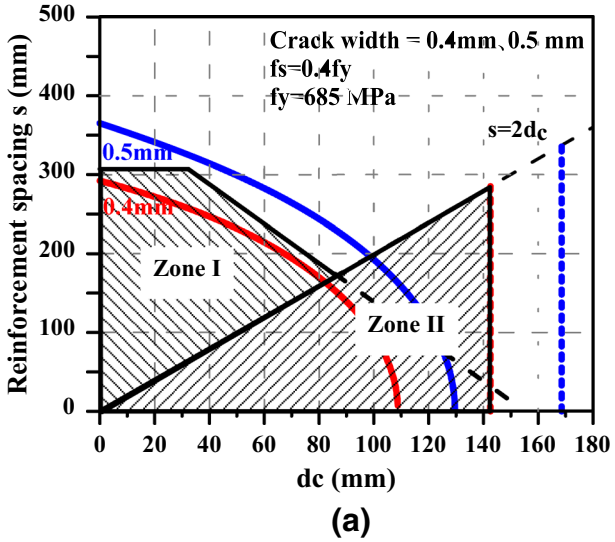

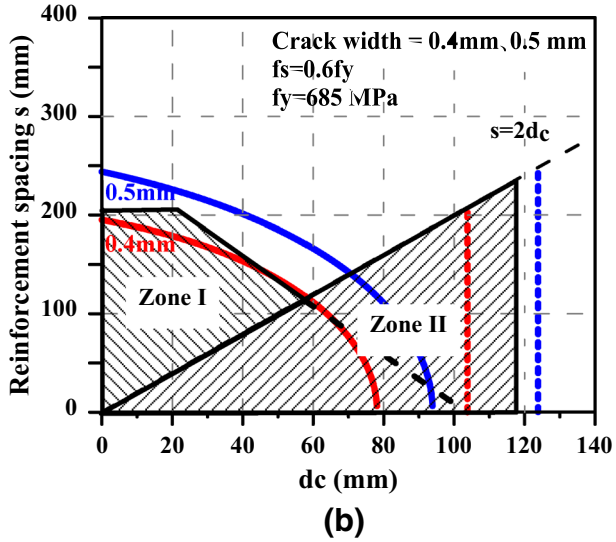

Fig. 20 Deign equations in ACI 318-14 for the flexural crack width control. **a** $f_s = 0.4f_y$ and **b** $f_s = 0.6f_y$.

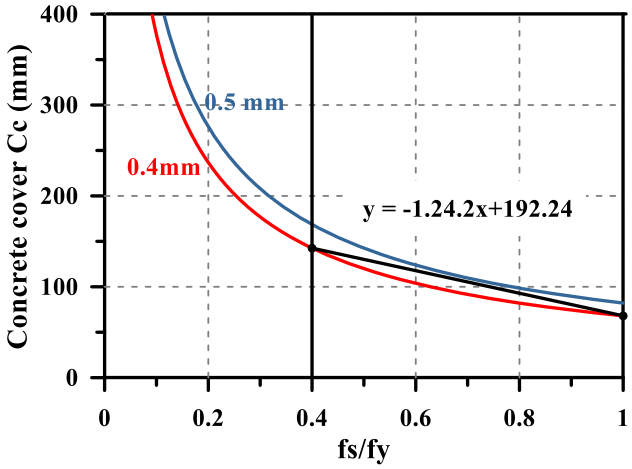

Fig. 21 Simplified equation for the maximum value of d_c.

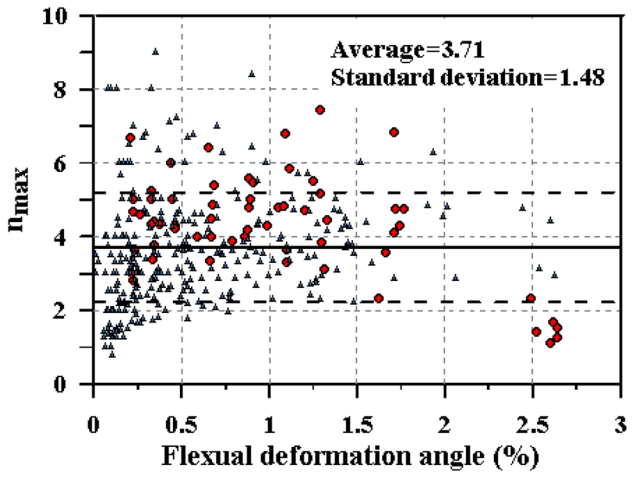

Fig. 22 Ratios of the maximum flexural crack width at the peak deformation angle and residual maximum flexural crack width (Circle points are the specimens in this work; triangle points are the specimens in the references (Chiu et al. 2014, 2016)).

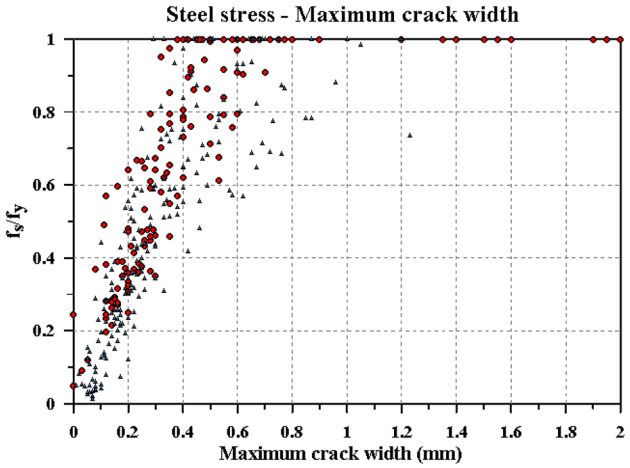

Fig. 23 Relationship between the maximum flexural crack width and maximum tensile stress of main bars (Circle points are the specimens in this work; triangle points are the specimens in the references (Chiu et al. 2014, 2016)).

between the maximum flexural crack width and the maximum stress of the tensile reinforcement, the latter reaches the yielding stress before the maximum flexural crack width exceeds 0.8 mm. Therefore, to ensure the reparability of an HSRC beam member in a medium-magnitude earthquake, the allowable tensile stress of the main bars can be set at the specified yielding stress of 685 MPa.

Since the specimens are all designed with the high-strength reinforcing bars with specified yielding stresses of 685 MPa (main bars) and 785 MPa (transverse reinforcement) and the high-strength concrete with the compressive strength of 70 or 100 MPa (measured compressive strength is in the range of 70–133 MPa), the proposed equations herein are applicable in the flexural crack control for HSRC beams. In the future, the experimental data of concrete and reinforcement with various strength should be added to extend the application of the proposed models.

Open Access

References

ACI Committee 318. (2002). *Building Code Requirements for Structural Concrete and Commentary*. Farmington Hills, Mich: American Concrete Institute.

ACI Committee 318. (2014). *Building Code Requirements for Structural Concrete and Commentary*. Farmington Hills, Mich: American Concrete Institute.

ACI Committee 363. (2010). *Report on high-strength concrete*. Farmington Hills, Mich: American Concrete Institute.

AIJ. (2010). *Standard for structural calculation of reinforced concrete structures*. Tokyo: Architectural Institute of Japan.

Chiu, C. K., Chi, K. N., & Lin, F. C. (2014). Experimental investigation on the shear crack development of shear-critical high-strength reinforced concrete beams. *Journal of Advanced Concrete Technology, 12*(7), 223–238.

Chiu, C. K., Sihotang, F. M. F., & Hao, D. (2015). Crack-based damage assessment method for HSRC shear-critical beams and columns. *Advances in Structural Engineering, 18*(1), 119–135.

Chiu, C. K., Ueda, T., Chi, K. N., & Chen, S. Q. (2016). Shear crack control for high strength reinforced concrete beams considering the effect of shear-span to depth ratio of member. *International Journal of Concrete Structures and Materials, 10*(4), 407–424.

FIB. (2010). *fib model code for concrete structures*. Paris: The International Federation for Structural Concrete.

FIP/CEB. (1990). *High strength concrete, State of the art report*. Bulletin d'Information No. 197, London, UK.

Frosch, R. J. (1999). Another look at cracking control in reinforced concrete. *ACI Structural Journal, 96*(3), 437–442.

Ho, B. T. (2018). *Study on the cracking control design for high strength RC beams*. National Taiwan University of Science and Technology (Master thesis), Taipei, Taiwan.

JSCE. (2007). Standard specifications for concrete structure Design. *Japan Society of Civil Engineers*. Tokyo, Japan.

Shimazaki, K. (2009). Evaluation of shear crack width based on shear force ratio. *AIJ Journal of Technology and Design, 15*(29), 139–142 **(in Japanese)**.

Silva, S. D., Mutsuyoshi, H., & Witchukreangkrai, E. (2008). Evaluation of shear crack width in I-shaped prestressed reinforced concrete beams. *Journal of Advanced Concrete Technology, 6*(3), 443–458.

Soltani, A., Harries, K. A., & Shahrooz, B. M. (2013). Crack opening behavior of concrete reinforced with high strength reinforcing steel. *International Journal of Concrete Structures and Materials, 7*(4), 253–264.

Zakaria, M., Ueda, T., Wu, Z., & Liang, M. (2009). Experimental investigation on shear cracking behavior in reinforced concrete beams with shear reinforcement. *Journal of Advanced Concrete Technology, 7*(1), 79–96.

Zhao, W. J., & Maruyama, K. (2004). Reevaluation of present equations for flexural crack width of RC beams. *Journal of Japan Society of Civil Engineers (JSCE), 490,* 147–156 **(in Japanese)**.